VTT Technical Research Centre of Finland

A screen-printed Ag/AgCl reference electrode with long-term stability for electroanalytical applications

Dawkins, Rebecca C; Wen, Dingchen; Hart, Judy N; Vepsäläinen, Mikko

Published in:
Electrochimica Acta

DOI:
10.1016/j.electacta.2021.139043

Published: 10/10/2021

Document Version
Publisher's final version

Electrochimica Acta 393 (2021) 139043

Contents lists available at ScienceDirect

Electrochimica Acta

journal homepage: www.elsevier.com/locate/electacta

A screen-printed Ag/AgCl reference electrode with long-term stability for electroanalytical applications

Rebecca C. Dawkins[a,b], Dingchen Wen[a], Judy N. Hart[b], Mikko Vepsäläinen[a,c,*]

[a] Mineral Resources, CSIRO, Private Bag 10, Clayton South, VIC 3169, Australia
[b] School of Materials Science and Engineering, UNSW Sydney, NSW 2052, Australia
[c] VTT Technical Research Centre of Finland, P.O. Box 1000, FI-02044 VTT, Finland

ARTICLE INFO

Article history:
Received 5 January 2021
Revised 2 August 2021
Accepted 2 August 2021
Available online 10 August 2021

Keywords:
Screen printed electrodes
Reference electrode
PDMS
Electroanalytical sensors
Silver/silver chloride

ABSTRACT

Low-cost sensor arrays are required to allow for real-time, *in-situ* electrochemical monitoring using Internet-of-Things (IoT) systems; however, they are currently not practical due to a lack of stable, mass-producible reference electrodes. To solve this problem, in this work we have developed a screen-printed Ag/AgCl true reference electrode with an offset salt reservoir on a flexible substrate for use in disposable, low-cost sensor arrays. A KCl-containing poly(vinyl acetate) ink was prepared as the solid-state electrolyte, and a PDMS junction membrane was deposited to suppress electrolyte leaching. The potentials of the electrodes with and without the electrolyte and junction membranes were measured versus a commercial saturated calomel reference electrode (SCE) in 0.1 M K_2SO_4 solution. Potential stability of -45.5 ± 3 mV vs. SCE with low drift was maintained for up to 27 days for electrodes containing both the electrolyte and PDMS layers, compared to less than 1 day without the PDMS junction. The electrodes were found to be stable in solutions at different pH and were also insensitive to most interfering ionic species, including SO_4^{2-}, I^-, Br^-, Cl^-, F^-, Li^+, Na^+, and K^+, under continuous potential measurement with an impedance of $\sim$ 15 kΩ at 106 Hz. The results demonstrate that the present printed reference electrodes are stable for an extended period and therefore well suited for use in electroanalytical systems for high volume IoT applications.

1. Introduction

Over the past decade, the growth in Internet-of-Things (IoT) technologies has brought the possibility of cheap and constant monitoring into a wider variety of natural and industrial environments [1]. Electrochemical sensing is extremely useful in multiple settings from environmental monitoring, to food and beverage quality control, and in medical devices. The development of reliable, low-cost new electrode technologies is necessary to fully realize the potential for real-time, *in-situ* IoT systems across the variety of electrochemical monitoring applications. Potentiometric and voltammetric systems can be used to detect a variety of analytes quickly and accurately, for example by measuring key water quality indicators such as pH and dissolved oxygen using ion-selective electrodes (ISEs) [2,3]. Systems based on ISEs require a stable reference electrode (RE) to reliably measure changes in ISE potential. Silver-silver chloride (Ag/AgCl) electrodes are a common choice due to their practical, simple, effective, and stable design [4]. The Ag/AgCl electrode potential is highly sensitive to Cl^- ion concentration ($[Cl^-]$), exhibiting a strong Nernstian response of −59.16 mV/pCl. A traditional Ag/AgCl reference electrode, commonly contained in a glass tube, suppresses this behavior by immersing an AgCl-coated Ag wire in a potassium chloride (KCl) electrolyte of known constant concentration, which is separated from the analyte solution via a porous junction or membrane. Maintaining electrolyte $[Cl^-]$ around the Ag/AgCl electrode in this way ensures the constant potential required for a stable reference electrode in the majority of solutions [5].

However, the fragile, rigid, and bulky construction of the traditional glass electrodes, as well as their high maintenance requirements, renders them unsuitable for many *in-situ* applications [6,7]. Thus, there has been significant interest in fabricating planar, all-solid-state Ag/AgCl screen-printed reference electrodes (SPREs) as a replacement. Screen printing is an inherently low-cost construction technique due to the wide choice of substrates, minimal

Abbreviations: IoT, Internet-of-Things; PVAc, Poly(vinyl acetate); EDS, Energy dispersive X-ray spectroscopy; SPRE, Screen printed reference electrode; AA, ascorbic acid; PP, Potassium permanganate.

* Corresponding author at: VTT Technical Research Centre of Finland, P.O. Box 1000, FI-02044 VTT, Finland
E-mail address: mikko.vepsalainen@vtt.fi (M. Vepsäläinen).

https://doi.org/10.1016/j.electacta.2021.139043

use of printing materials, and the scalability for mass-production with minimal labor required [8–10]. The choice of and precise control over both product dimensions and materials that is possible through screen printing has meant that SPREs are expected to facilitate the development of commercially-viable rugged, robust, flexible, portable, miniaturized, and disposable low-cost sensors suitable for *in-situ* measurement [11]. Due to the difficulty of converting the electrolyte to a stable printable form, many SPREs fabricated in the past have been Ag/AgCl pseudo-reference electrodes (pseudo-REs) without an internal electrolyte [9,12–14]. In some voltammetric measurements precise control of the potential from a RE is less crucial, and a pseudo-RE may be sufficient [15,16]. However, the high sensitivity and consequent potential instability of bare Ag/AgCl to [Cl^-] and other interfering species renders these pseudo-REs useful only under controlled or well-defined conditions and standard REs are often preferred in both potentiometric and voltammetric measurements [5,16,17].

Therefore, recent developments have focused on fabricating reliable Ag/AgCl SPREs incorporating an inner electrolyte layer to provide constant ionic activity once hydrated. This concept is commonly used in all-solid-state REs to excellent effect, and often involves a UV-cured cross-linked [18–20] or injection molded [21] poly(vinyl acetate) (PVAc) and KCl mixture, or pure KCl melt [22]. These materials are yet to be translated to a printed medium. In previous work, a printed inner electrolyte layer has been made from a paste typically containing KCl powder mixed with a glass [7,23], gel [8,24–26], or polymer-based composite [13,27,28], although conductive polymers [29], ionic liquids [30], and charge-balanced lipophilic salts [31] have also been investigated. In each of these previous studies, the electrolyte layer extended the electrode lifetime and reduced cross-sensitivity, especially where Cl^- was absent from the analyte solution. However, leaching of the small electrolyte reserve around the Ag/AgCl layer to surrounding solution can induce electrode potential drift and eventual failure as the internal [Cl^-] is locally depleted [32]. An additional study by Glanc et al. [28] further reduced [Cl^-] susceptibility by overprinting a secondary electrolyte layer, emulating the traditional, stable double-junction RE.

Separation of the inner electrolyte from the analyte solution via a liquid junction has been found to increase Cl^- retention [28], resulting in lower drift rates and longer lifetimes than electrodes without this component [9]. Shitanda et al. [27] incorporated a printed channel of poly(dimethyl siloxane) (PDMS) and poly(ethylene glycol) emulsion as a liquid junction, achieving electrode lifetimes beyond 70 days; however, this additional barrier increased the hydration time required to obtain a stable potential. Subsequent investigation into the dual-use of a porous paper substrate as both liquid junction and electrolyte reservoir reduced the hydration time to 1 min, albeit with a much shorter lifetime of 3 days [33]. Recently, Komoda et al. [24] achieved hydration in 3 min whilst maintaining a reasonable lifetime of 21 days by using a liquid junction consisting of a silica gel and poly(vinylidene difluoride) mixture. There are few examples of SPREs with long, stable lifetimes, and very little research into their viability in a range of chemical environments.

This paper presents a flexible, low-cost SPRE with a simple construction (Fig. 1). Electrodes were fabricated on PET substrates using screen printing, and consist of (1) a printed electrolyte layer containing KCl and PVAc over the Ag/AgCl layer, which functions as both a conducting and sensing layer, (2) a PDMS membrane acting as a liquid junction, and (3) a dielectric protective coating. The Ag/AgCl sensing layer and the working area as defined by the dielectric coating were offset, with the electrolyte and junction layers in between, creating an extended reservoir to encourage constant Cl^- saturation around the sensing layer. The overall design is similar to those presented by Glanc et al. [28] but is differentiated from previous work by the offset between the sensing layer and working area, whereas the electrodes reported by Glanc et al. [28] had the junction and electrolyte layers directly over the sensing layer, and those reported by the research group of Shitanda [24,27,33] had a junction channel in contact with both the electrolyte and sensing layers. The lifetimes achievable with this construction, as well as the cross-sensitivity of the developed electrode to halogen, alkali, and sulfate ions as well as various redox species and pH environments, are investigated.

2. Materials and methods

2.1. Materials

Silver-silver chloride (Ag/AgCl) ink (124–36) and solvent-resistant dielectric ink (118–08) were purchased from Creative Materials Inc. (USA). Polydimethylsiloxane (PDMS) Sylgard 184 Elastomer Kit was purchased from Dow Corning. Polyethylene terephthalate (PET) film was purchased from Vic Plastics (AUS). For the electrolyte ink, potassium chloride (KCl) was purchased from Merck (min. assay 99.5%), poly(vinyl acetate) (PVAc, 1,00,000 MW) from Aldrich, and analytical grade acetone from Merck. pH buffers used in electrode testing were purchased from Merck. Ultrapure water obtained from a Millipore Milli-Q purification system was used throughout this work.

2.2. Ink preparation

The KCl crystals were ring milled for 30 s to create a fine powder. The electrolyte ink (KCl/PVAc) was then prepared by mixing 15 g KCl powder, 7.5 g PVAc, and 25 mL acetone using a magnetic stirrer overnight. All commercial inks were prepared according to the manufacturer's instructions.

2.3. Electrode fabrication

The electrodes were fabricated by standard screen-printing techniques using a semi-automatic screen printer (Devil Label Printer, TAS International, AUS) and stainless-steel mesh screens. First, the Ag/AgCl layer (5 × 47 mm) was printed onto the 125 µm thick PET substrate and cured for 30 min at 100 °C. Next, the KCl/PVAc ink was printed (7 × 45 mm); as described below, this layer was printed either two or four times to test the effect of electrolyte thickness on performance, and was air-dried for 15 min at room temperature between prints. Subsequently, the PDMS membrane layer (7 × 45 mm) was printed and cured at 100 °C for 35 min. Finally, the dielectric insulating layer (10 × 50 mm, with a 5 × 5 mm window exposing the underlying layers) was printed and cured at 100 °C for 1 h. Both the PDMS membrane layer and the dielectric layer were printed and cured twice to ensure full coverage of the electrode surface. The position of the dielectric layer window was offset such that it began at the edge of the Ag/AgCl layer (Fig. 1) to create an electrolyte reservoir between the analyte and the Ag/AgCl layer. Each print batch manufactured 12 electrodes simultaneously onto the substrate sheet.

Electrodes with various layer structures were manufactured for lifetime comparative testing. Each structure retained the Ag/AgCl and dielectric layers as described above, with the pseudo-reference electrode (0N) containing these layers only. Electrodes were also prepared with the KCl/PVAc electrolyte layer printed either two (2N) or four (4N) times and no PDMS layer, or with two (2P) or four (4P) electrolyte prints and a PDMS layer. The structure of the 4P electrode is illustrated in Fig. 1 as an example; images of the electrode at each step of fabrication and the completed electrode are shown in Supplementary Information (Fig. S1).

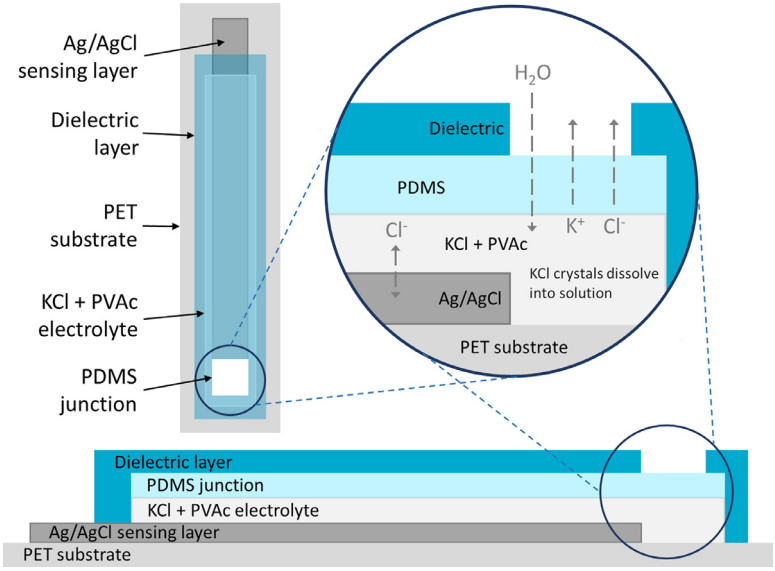

Fig. 1. Structure and composition of the 4P SPRE; inset illustrates the ionic exchange pathways within the electrode, and between electrode and analyte.

2.4. Performance testing and electrode characterization

2.4.1. Lifetime testing

Open circuit potential (OCP) was used to compare the lifetime, stability, and reproducibility of the different SPRE structures. Five replicates of each electrode design (0N, 2N, 4N, 2P, 4P) from the same print batch were tested, and replicate sets from additional print batches were also tested for the 4N and 4P designs (4Nr, 4Pr). OCP was measured at 25 °C in a 0.1 M K_2SO_4 analyte solution which was replaced every 7 days (Test 1). During the repeated experiment (Test 2) the solution was not replaced, and instead fresh solution was added after ~2 months to compensate for evaporation of the analyte. The experiment was set-up in a two-electrode system, with the SPRE as the working electrode (WE) and a saturated calomel electrode (SCE) (1001 Series SCE, Koslow) as the RE. Measurements were made using a Keysight 34972A LXI Data Logger Switch Unit with a 34901A Multiplexer. The electrodes were attached to wire leads using RS PRO Silver Conductive Adhesive Epoxy and the connection points, which were not immersed in the analyte solutions, were protected using a stop-off lacquer (Fortolac, Ami-Con). All potential values are reported against SCE.

2.4.2. Interference testing

Interference testing was undertaken to determine the stability of the 4P-SPRE electrodes in different solutions. The suppliers and purities of the materials used throughout the experiments are documented in Table S1. For the alkali tests, 0.1 M solutions of K_2SO_4, Na_2SO_4, and $Li_2SO_4{\cdot}H_2O$ were prepared, and 0.1 M solutions of KI, KBr, KCl, and KF were used for the halogen ion test. For the redox test, 0.1 M and 0.01 M solutions of ascorbic acid and $KMnO_4$ were prepared. In addition, performance was also measured in solutions of H_2O_2 at 0.01 M, 0.1 M, and 1 M in 0.1 M K_2SO_4. Solutions of 10% w/v KOH and 10% v/v H_2SO_4 were made for the acid/base test; the electrodes were placed in 0.1 M K_2SO_4 in between testing in these strong acid and base solutions to minimize neutralization reaction effects. For the pH test, buffers at pH 4, pH 7, and pH 10 were used. For testing sensitivity to Cl^- and SO_4^{2-}, KCl solutions at concentrations of 0.001 M, 0.01 M, 0.1 M, 1 M, and saturated (~3.4 M) and K_2SO_4 solutions at 0.1 M, 0.2 M, 0.4 M, and saturated (~0.7 M) were prepared.

For each interference test, a set of five SPRE replicates was placed in the solutions sequentially, with a period of 1–6 days in each solution. For the alkali solutions, an experiment which reversed the testing order for the solutions was also performed. All tests started with a fresh SPRE set, except the KCl concentration and H_2O_2 tests which used SPREs from the 'reverse' alkali and redox tests, respectively. The pH, H_2O_2, and KCl concentration tests were continued to the point of electrode failure (in pH 4 or 0.1 M K_2SO_4 solutions, respectively, once interference data collection was complete); the remaining tests were stopped once testing was completed satisfactorily in all solutions. All tests were undertaken at 25 °C in approximately 60 mL of solution.

Electrode impedance and OCP were measured for the interference tests using a multi-channel potentiostat (BioLogic VMP3, ProDigitek, AUS). The SPREs, once connected to leads as described in Section 2.4.1, were used as WEs in a three-electrode system alongside a platinum wire counter electrode (CE) and SCE RE.

Due to the extended nature of testing, which lasted for up to 50 days, occasional maintenance, connection, and hardware issues resulted in missing or incomplete data, which has been removed from subsequent analysis.

2.4.3. Structural morphology and composition

The cross-sectional structures and chemical compositions of the 4P and 4Pr electrodes were analyzed both prior to lifetime testing and post-failure. Sample preparation involved cutting and mounting in epoxy, polishing using an oil-based suspension to minimize KCl dissolution, and finally vacuum coating with carbon (BOC Edwards Auto 306). A scanning electron microscope (SEM) equipped with an energy dispersive X-ray spectroscope was used (FEI Quanta 400 F).

2.5. Application testing

2.5.1. Stability in real solutions

The long-term stability of the 4P SPRE was tested in three representative samples – tap water, creek water, and coffee. Each test measured OCP via a potentiostat (BioLogic VMP3) using a three-electrode system. Three 4P SPRE replicates were tested as the WEs with a platinum CE and SCE RE in each of the chosen solutions. The coffee solution was replaced on Day 16, and all tests were terminated after 30 days.

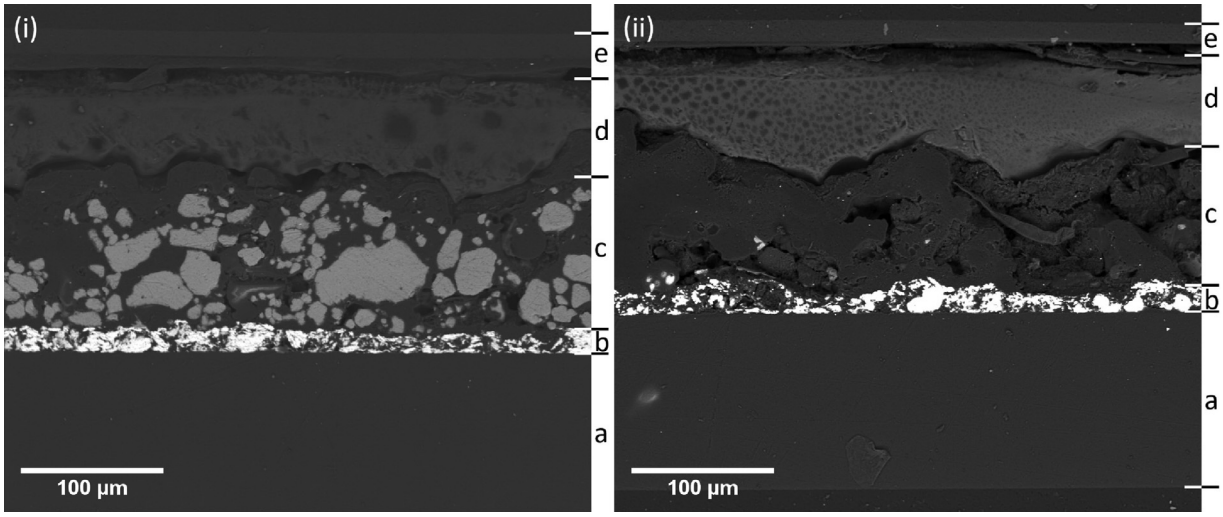

Fig. 2. SEM cross-sectional images of 4Pr (i) prior to, and (ii) post lifetime testing in 0.1 M K_2SO_4 solution: (a) PET substrate, (b) Ag/AgCl layer, (c) KCl/PVAc electrolyte layer, (d) PDMS layer, and (e) dielectric layer.

2.5.2. pH probe tests

Potential measurements were conducted via a potentiostat (biological VMP3) using a two-electrode system involving a commercial glass pH electrode (InLab Expert Go-ISM, Mettler Toledo) as a WE and a 4P SPRE as an external RE, which had been preconditioned for 2 h in 0.1 M KCl. The potential measurements were performed for 5 min at ambient temperature in each of eight pH buffers (pH 1, 2, 3, 4, 7, 8, 9, 10) in ascending and descending (reverse) order to establish a calibration curve. This calibration curve was used to determine the pH of six representative samples – tap water, carbonated tap water, creek water, coffee, milk, and orange juice samples. For comparison, the pH of the six samples was also measured using the glass pH probe and its internal reference electrode via a pH meter (SevenGo Duo Pro, Mettler Toledo).

2.5.3. Cyclic voltammetry

A PalmSens3 potentiostat (PalmSens) controlled by PSTrace 5.5 software was used to perform cyclic voltammetry measurements with a standard three-electrode configuration. The 1 mm glassy carbon disk (ET074, eDAQ) WE was measured against a SCE or a 4P SPRE using a platinum wire as CE. Prior to use, the WE was polished on a PSU-MM polishing pad (Kemet) using 6-KD-C3 diamond paste (Kemet), then rinsed with ethanol and dried. All voltammograms were performed in a 2 mM $[Ru(NH_3)_6]Cl_3$ solution containing a 0.1 M KNO_3 supporting electrolyte, with scan rates of 10 to 100 mV/s.

3. Results and discussion

3.1. Structural characterization

SEM was used to analyze the printed layers and determine their thicknesses. Both the 4P and 4Pr samples imaged were similar, and the SEM images for 4Pr are shown in Fig. 2. The thicknesses of the electrolyte and PDMS layers varied significantly across each sample due to the coarseness of the KCl crystals, which comprised 34% v/v of the electrolyte layer and range from < 2 to 75 µm in diameter (Fig. 2(i)). The 'valleys' between the KCl particles are subsequently filled by the liquid PDMS, leaving a relatively smooth surface at the top of the PDMS layer. The PDMS layer also appears to have retained a substantial amount of microcavities from the printing process.

The total thickness of ~224 µm for all the printed layers is substantially greater than in previous studies [24,27,28], despite similar print dimensions, due to the repeat prints and larger screen mesh size used in this study. The observed thickness was reduced to 202 µm (Fig. 2(ii)) post-failure (after 50 days in 0.1 M K_2SO_4). The majority of this change occurred within the electrolyte layer and is attributed to the KCl particles leaching and dissolving into solution, creating voids (evident in Fig. 2(ii)) which later collapsed. Energy-dispersive X-ray spectroscopy (EDS) analysis also indicated an absence of K and Cl in the electrolyte layer post-failure, while the composition of the other layers remained unchanged (Figs. S2–4).

3.2. Lifetime testing

The performance of SPREs with different structures was compared over their lifetimes through OCP measurement in 0.1 M K_2SO_4. Five replicates of each electrode design (0N, 2N, 4N, 2P, 4P) were tested alongside replicates from separate 4N and 4P print batches, denoted by 'r'; the electrodes were not conditioned prior to measurement. Test 2 included the 0N, 4N, 2P, 4P, and 4Pr electrodes only.

Hydration time was defined as the time taken for the electrode potential to stabilize at −45 ± 5 mV vs. SCE. Similarly, failure was defined as the point where the electrode potential drifted beyond −45 ± 5 mV vs. SCE, which is the common stability range for commercial REs applied in electroanalytical applications. Short excursions outside this range were not considered failure if the potential returned to and stabilized in the accepted range within 24 h. Table 1 shows a summary of electrode performance. Fig. 3 shows the operational potential for the tested SPREs averaged over the replicates tested. The failure time for each replicate is indicated in Fig. 3; the electrodes were excluded from the average potential once they were considered to have failed.

The 'bare' pseudo-REs (0N) did not reach the theoretical potential of −45 mV vs. SCE for Ag/AgCl at any time during the test, instead stabilizing at 114 ± 36 mV vs. SCE within 15 h. A similar result was obtained for the SPREs fabricated with two electrolyte print layers (2N), which stabilized within the first 15 h at 98 ± 44 mV vs. SCE and never reached −45 mV vs. SCE. The addition of two further electrolyte print layers in the 4N and 4Nr electrodes did allow potential stabilization at −45 mV vs. SCE, with lifetimes in Test 1 of less than 15 h for 4N and up to 16.5 h for 4Nr samples. More frequent sampling in the early stages of Test 2 revealed that the 4N electrodes reached hydration within 2 min

Table 1
Comparison of OCP response for various electrode structures. All values are given as sample mean ($\bar{x}$) ± standard deviation (σ) for the batch of n replicate electrodes, except potential drift which uses standard error, for the combined results from Tests 1 to 2. Additional information is included in Table S2. ^Test 2 only ^^Test 1 only *Data only reported for 8 electrodes, as 2 outliers (Test 2) were excluded from the analysis.

Type	Electrode structure	*n*	Working potential (mV vs. SCE)	Hydration time^ (min)	Potential drift (mV/day)	Lifetime (days)
0N	Ag/AgClDielectric	10	–	–	–	< 0.01
2N	Ag/AgCl, 2 × electrolyte, Dielectric	5	–	–	–	< 0.63
4N	Ag/AgCl, 4 × electrolyte, Dielectric	5^	−47.29 ± 2.51	1.23 ± 0.37	97.38 ± 11.28	0.05 ± 0.02
4Nr	Ag/AgCl, 4 × electrolyte, Dielectric	2^^	−40.82 ± 0.43	–	18.92 ± 4.58	~ 0.63
2P	Ag/AgCl, 2 × electrolyte, PDMS, Dielectric	10	−45.67 ± 1.61	9.55 ± 4.47	0.172 ± 0.002	15.43 ± 3.05
4P	Ag/AgCl, 4 × electrolyte, PDMS, Dielectric	10	−45.95 ± 2.58	13.44 ± 11.11	0.254 ± 0.003	15.83 ± 2.62
4Pr	Ag/AgCl, 4 × electrolyte, PDMS, Dielectric	8*	−45.29 ± 2.64	38.22 ± 37.86	0.047 ± 0.002	27.09 ± 6.78

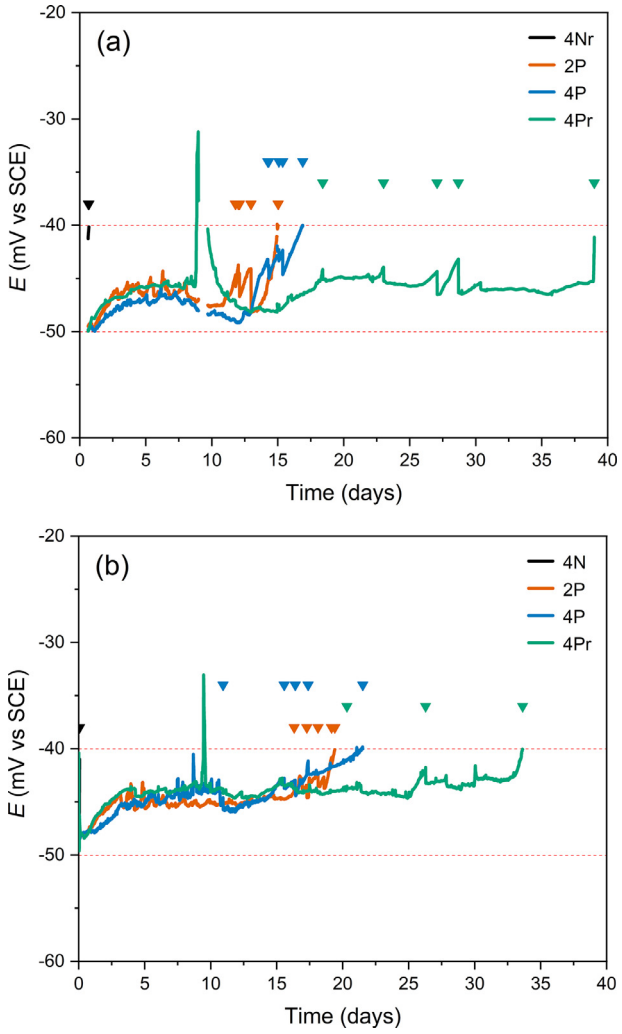

Fig. 3. Average electrode potential (E) over the operational electrode lifetime during OCP measurements for the batch of replicate electrodes of each type: (a) Test 1, (b) Test 2. Arrows (▼) represent the failure times for each electrode. Dotted red lines at −40 mV and −50 mV vs. SCE indicate the failure conditions used in this study. Hydration curves are not shown for clarity, and individual electrode data was excluded after failure. Data was not recorded during the first 15 h of Test 1 (a). An excursion in electrode potential (to +31 mV) was seen for one 4Pr sample in Test 1, which stabilised again inside the operational range (-45 ± 5 mV vs. SCE) within 2 days; this is thought to have originated from a surface bubble and was not considered electrode failure.

at −49.8 ± 5.0 mV vs. SCE and continued working for another 1.2 ± 0.4 h prior to considerable drift (97.4 mV/day) indicating failure.

Significantly, long lifetimes of 15–27 days and low drift rates (0.25–0.05 mV/day) were observed for all electrodes with a PDMS junction over the electrolyte layer (*i.e.* the 'P'-type SPREs: 2P, 4P, 4Pr) (Table 1). The 4Pr samples displayed the lowest potential variability prior to failure out of all samples tested, and a considerably lower drift rate (0.05 mV/day) compared to the previously reported lowest rate of 4.8 mV/day [9] for fully screen-printed Ag/AgCl REs [23,34]. While the addition of a barrier between the electrolyte and analyte has been known to increase the lifetime of a SPRE, this often comes at the expense of an extended hydration time. Despite the hydration time being extended by the PDMS junction layer, it remains short (10–40 min) relative to the operational SPRE lifetimes reported here, as well as among previous studies demonstrating long lifetimes [23,27,28,30] over a period of days to weeks.

Throughout both tests it became apparent that electrode drift for the 'P'-type SPREs fell into two distinct sections, with appreciably higher drift rates over the initial 3 to 4 days (*i.e.* 1.49 mV/day for 4Pr, Fig. 3), following which the drift rate reduced markedly for the remainder of their lifetimes (*i.e.* to 0.02 mV/day for 4Pr). This suggests that an additional, more subtle hydration equilibration process is completed over the first 3 to 4 days in solution, which affects the SPRE potential during continued minor dilution in the electrolyte layer.

Characteristically, failure of all tested SPREs began with a sudden rise in potential which creates a 'ramp' in the batch average in Fig. 3, consistent with the Nernstian response of Ag/AgCl upon local [Cl^-] dilution. KCl particle loss was demonstrated as the biggest compositional change through post-failure SEM and EDS analysis (Fig. 2 and Figs. S2–4), further supporting consistent KCl loss until complete depletion as the likely cause of electrode failure, with subsequent exposure to [Cl^-] variations destabilizing the underlying Ag/AgCl (evidenced by the sudden changes in potential of the 'N'-type electrodes that were observed when the analyte solution was replaced weekly in Test 1). According to the results, the hydrophobic PDMS layer on top of the KCl-PVAc composite layer ('P'-type electrodes) can reduce electrolyte loss and improve the lifetime and potential stability of the electrode. Although PDMS is moderately hydrophobic and acts to restrict the passage of water molecules, it remains slightly permeable to water (diffusion coefficient 2 × 10^{-9} m^2/s) [35]. The combination of this slight permeability with the microcavities in the PDMS layer observed by SEM analysis (Fig. 2) provides sufficient diffusion pathways through the PDMS membrane for ion exchange, completing the electrochemical cell while retaining a physical and chemical barrier minimising Cl^- loss [36]. This effect is further strengthened by the presence of an electrolyte reservoir between the Ag/AgCl layer and analyte solution, created by offsetting the working area and the Ag/AgCl layer, which works with the overlying PDMS junction membrane to ensure a constant electrolyte concentration to maintain potential stability. In further support of this, the potentials of the 'P'-type electrodes were not significantly affected by weekly solution changes in Test 1 (in contrast to the 'N'-type electrodes), which can be attributed to the PDMS layer and the offset electrolyte reservoir slowing KCl leaching, ensuring a constant [Cl^-] and hence electrode potential despite changes in the analyte composition. Further

work is required to determine the effect of any undesired biofouling due to the hydrophobic PDMS surface [37].

Many previous studies have reported electrode lifetime as the operational time during which the potential drifted by no more than 30 mV, as defined by Shitanda et al. [27]. Using this definition (i.e. potential maintained within −45 ± 30 mV vs. SCE), the mean SPRE lifetimes in this study would be greater than 37 days for the 4P-type electrodes and 29 days for 2P, with 60% of the 'P'-type electrodes in Test 2 considered operational even at the termination of data collection (70 days). This places both the 2P and 4Pr SPREs among the longest lifetimes reported in the literature for thick-film Ag/AgCl REs [12,23–25,27,30,38]. Even using the tighter tolerance on potential drift of ± 5 mV, which is more appropriate for practical electroanalytical applications, the stable lifetimes as reported here are similar to those reported in leading studies. It should be noted that in Test 2, in which the analyte solution was not replaced during the ~2 month test period but was simply topped up as required to compensate for evaporation of the analyte, the change in solution concentration due to complete KCl salt leaching is estimated to be < 0.025 M KCl in 0.1 M K_2SO_4, which would have a negligible effect on the SPRE potential and hence the evaluated lifetime.

Overall, for the electrode structure reported here, translating the high-performing PVAc and KCl matrix from previous all-solid-state REs to a screen-printed PVAc-KCl composite layer, improves the lifetime and the potential stability of the electrodes by providing a constant [Cl^-] environment. This effect was enhanced through offsetting the electrode working area, which creates an electrolyte reservoir 'buffer' between the analyte and the sensing layer. The addition of the PDMS layer further reduces KCl loss from the offset electrolyte reservoir as well as ion diffusion from the analyte into the reference electrode, further improving the SPRE performance.

3.3. Interference testing

3.3.1. Interference species

To determine the SPRE response to various interfering species, multiple tests were carried out for three species types, with each test using a fresh batch of five 4P electrodes: (1) substitutional halide and alkali ion species, (2) strong redox agents, and (3) acids and bases. The electrodes were tested for a minimum of 1 day under each interference condition. The results are shown in Fig. 4, with additional information in Table S3.

In the substitutional halide ion test involving I^-, Br^-, Cl^-, and F^- (Fig. 4(i), Fig. S5), the difference in potential exhibited by the SPREs across the anionic species was minor (< ± 1 mV) and within the operational potential range (*i.e.* −45 ± 5 mV vs. SCE). In contrast, previous studies [9,30,31] have demonstrated a moderate sensitivity to Br^- of up to ± 8 mV for thick-film REs without a junction layer, which further highlights the effectiveness of this layer.

The alkali ion tests, involving K^+, Na^+, and Li^+, were done in both a 'forward' (Fig. 4(ii)) and 'reverse' (i.e. Li^+, then Na^+ and K^+) (Fig. 4(iii)) order, using fresh SPREs in each case. The 'reverse' test was to confirm whether the minor potential drift evident in fresh electrodes over the initial 3–5 days of use, across multiple conditions, was due to inherent electrode processes or an artefact of the testing order of the investigated species. A positive drift was seen throughout the initial few days regardless of the order of species tested (1.9 mV/day for the 'forwards' test vs. 0.5 mV/day for the 'reverse' test), reinforcing that this drift is attributed to dilution upon progressive hydration of the electrolyte layer. The effect of species interference was difficult to isolate from this initial ~4 day dilution process, however any potential change between the alkali species was relatively low in both the 'forwards' and 'reverse' tests (< ± 3 mV and ± 1 mV change, respectively) and similar to the potential fluctuation observed in the SCE over the same period (± 2 mV). Slight drifting of the potential outside of the operational range (-45 ± 5 mV vs. SCE) by under 3.5 mV during the 'forwards' alkali test (Fig. 4(ii)), and its recovery soon after, was likely influenced by the SCE potential fluctuation mentioned above and is not considered SPRE failure.

In the redox test, one reductant (ascorbic acid) and two oxidant ($KMnO_4$ and H_2O_2) species were used (Fig. 4(viii) and (ix)) with a double junction for SCE stability. Initially, SPREs were tested alternately in ascorbic acid and $KMnO_4$ at 0.1 M and then 0.01 M, followed by testing in H_2O_2 (in a conductive 0.1 M K_2SO_4 support solution) at 0.01 M, 0.1 M, and 1 M. The formation of dark brown, clearly visible $KMnO_4$-related precipitates appeared to have a large impact on potential (−110 mV vs. SCE in the 0.1 M solution) by clogging the electrode and causing sluggish behavior [39], although further work is required to determine the mechanisms involved. H_2O_2 showed negligible effect on potential but caused significant noise at high concentrations, possibly due to bubbles formed upon H_2O_2 decomposition insulating the electrode surface and disrupting ionic exchange across the junction membrane. Therefore, we can conclude that specific oxidation by-products can have pronounced effects on SPRE potential, and that the effects differ depending on the oxidant or by-product involved, in line with previous reports [30,31]. Consistent with Tymecki et al. [9], reductants had less effect on electrode potential, with the electrode potential in ascorbic acid being within the expected range in the initial test and returning to it after exposure of the electrodes to $KMnO_4$ (albeit slowly after the second, longer exposure to $KMnO_4$).

The SPRE electrodes were also tested for stability at pH 4, pH 7, and pH 10 in both increasing and decreasing order (Fig. 4(vi)), with only minor changes in the SPRE potential of +0.29 mV/pH, compared to previous studies (±5 mV/pH [28], −3 mV/pH [40]), although there were some brief spikes in potential at pH 10.

To determine SPRE responses in extreme basic and acidic environments, testing was done in 10% solutions of KOH and H_2SO_4 (alternated with 0.1 M K_2SO_4 to minimize neutralisation reaction effects), with a double junction employed to improve SCE stability. The SPREs demonstrated some sensitivity to both species (Fig. 4(vii)), with potentials of −39.4 ± 2.4 mV vs. SCE for KOH and −53.5 ± 7.9 mV vs. SCE for H_2SO_4; the variation from the expected range of −45 ± 5 mV vs. SCE is small considering the high concentrations investigated.

Hydration times for fresh SPREs across these tests varied between 1 min and 2 h, which is consistent with the results for the same 4P electrodes in the lifetime tests (Table 1), and reasonably short relative to the SPRE lifetimes demonstrated in this study. Similarly consistent with the lifetime tests (Section 3.2), the dilution-induced positive drift (of < 2 mV/day) was again observed during the initial 3–5 days of most tests, except where large potential changes in the acid/base and redox tests obscured such subtle processes.

The pH and redox/H_2O_2 tests were continued until electrode failure (Figs. S7–8) using the criterion defined for lifetime testing (-45 ± 5 mV, Section 3.2). Electrode lifetimes of 26.0 ± 3.1 days were achieved at pH 4 prior to permanent potential drift, and one electrode from the redox/H_2O_2 test reached a lifetime of 91 days after being placed in 0.1 M K_2SO_4 (average 76.4 ± 12.5 days), despite significant interference from the redox species, which is the longest measured lifetime in this work. It is noteworthy that these results are consistent with those from the lifetime tests despite the vast differences in testing conditions.

3.3.2. Concentration effects

The effect of chloride interference was investigated for [Cl^-] from 10^{-3} M to saturated (~3.4 M) KCl using SPREs from the 're-

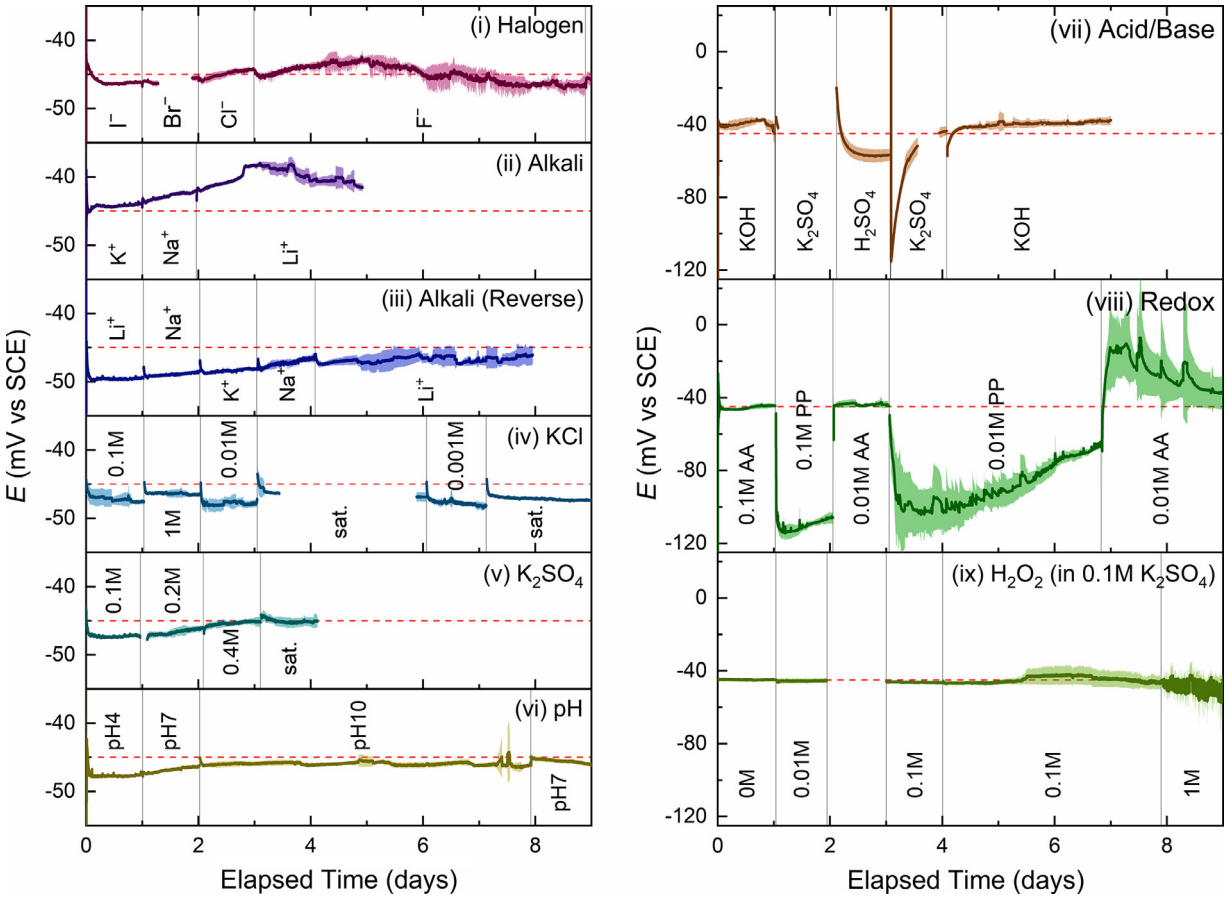

Fig. 4. Electrode potential responses of the SPREs during the initial 9 days of interference species tests; 5 replicate samples were tested for each species. Fresh electrodes were used in all but (iv) and (ix), which used the same electrodes as (iii) and (viii), respectively. Two SPREs failed to recover upon rehydration after exposure to $KMnO_4$, so only three electrodes were tested in H_2O_2. The dark solid lines represent the mean potentials, while the surrounding shaded regions indicate the potential range within one standard deviation (σ) of the mean. The dotted red line is displayed for clarity and indicates the theoretical Ag/AgCl/KCl RE potential of −45 mV vs. SCE. Gaps in the data are due to software or connection issues. Three electrodes in the first day of KOH testing (vii) were affected by physical disturbance of the test set-up, and the resultant potential spike has been removed from analysis. AA: ascorbic acid, PP: potassium permanganate ($KMnO_4$).

verse' alkali ion test; the solutions were tested in a randomized order. No notable dilution period was detected (Fig. 4(iv), Fig. S6). The SPRE sensitivity was −0.31 ± 0.15 mV/pCl, well within the common ± 5 mV error margin demonstrated by the commercial SCE RE used in this work and markedly better than for previously reported SPREs, which had susceptibilities to [Cl^-] between −2 and −10 mV/pCl [34,41]. Although a higher KCl concentration and additional epoxy-based junction layer has been reported to reduce sensitivity to −0.3 ± 10 mV/pCl, that electrode was not stable in saturated solutions [28]. In this work, the constant electrolyte concentration ensured by the working area and Ag/AgCl layer offset reservoir, combined with the overlying PDMS junction membrane, reduce [Cl^-] sensitivity of the SPRE and maintain potential stability, including up to solution saturation.

The effect of K_2SO_4 concentration in the range from 0.1 M to saturation (~0.7 M) was also investigated (Fig. 4(v)); it is difficult to discern a concentration influence from the underlying dilution period, but susceptibility is within the expected range and there is no notable effect of K_2SO_4 concentration on SPRE potential. This is consistent with previous studies on SO_4^{2-} sensitivity [8,27,30].

3.4. Electrochemical impedance

Reference electrode impedance can have undesirable effects on the performance of electroanalytical systems such as measurement noise or potentiostat oscillation especially during high-frequency or high-speed measurements [39]. Therefore, impedance magnitude (|*Z*|, Ω) at 106 Hz was used to evaluate these aspects of performance by indicating the initial rate of stabilization and ionic conductivity of the SPREs. All fresh electrodes demonstrated a significant decrease in |*Z*| to below 25 kΩ during an initial 3–11 h hydration and stabilization period, at a rate of between −7.8 and −83.7 kΩ/h depending on the initial impedance magnitude. In combination with the results from Section 3.3.1, this indicates that, although stabilization of the electrode's ionic conductivity takes slightly longer than potential stabilization upon hydration, this has no appreciable effects on potential. In the redox test, the OCP noise discussed in Section 3.3.1 aligns with increased impedance upon increasing H_2O_2 concentration and verifies that this behavior relates to insulation of the junction surface by O_2 gases from H_2O_2 decomposition. The electrodes' impedance after stabilization of ~15 kΩ in most tests is satisfactorily low, indicating sufficient electrode ionic conductivity to have negligible effect in electroanalytical applications [39].

3.5. Stability in real solutions

The performance and lifetime of the SPREs in real-world analytes were investigated over a 30-day period through OCP measurement of three replicate 4P SPRE electrodes in three common solutions – coffee, tap water, and creek water. The results for the best performing electrode from each test are shown in Fig. 5.

Table 2
Summary of OCP responses for 4P SPREs in a selection of common solutions. All values are given as sample mean ($\bar{x}$) ± standard deviation (σ) for the 3 replicate electrodes tested in each solution. Lifetime represents the time before the potential drifts permanently above –40 mV.

Test Solution	Hydration Time (min)	Working Potential (mV vs SCE)	Lifetime (days)
Tap Water	91.5 ± 98.9	−51.21 ± 5.86	16.39 ± 6.48
Coffee	18.3 ± 15.3	−52.40 ± 7.27	18.95 ± 8.43
Creek Water	13.3 ± 1.6	−51.74 ± 5.38	22.29 ± 2.17

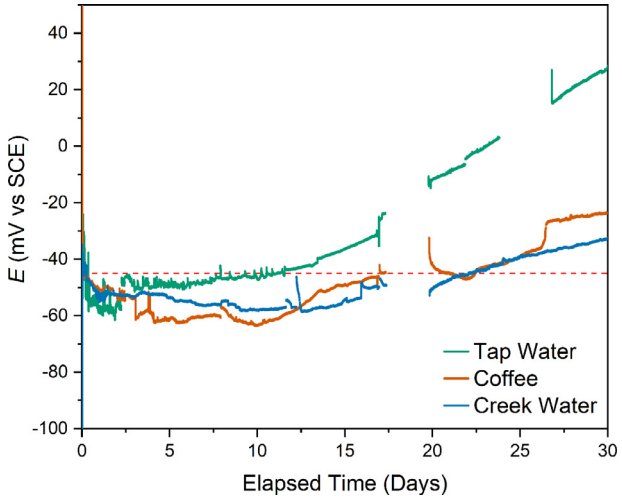

Fig. 5. Electrode potential response during OCP measurement for one 4P SPRE electrode in tap water (green), coffee (brown), and creek water (blue). The dotted red line indicates the theoretical Ag/AgCl/KCl RE potential of −45 mV vs. SCE. Gaps in the data are due to software issues.

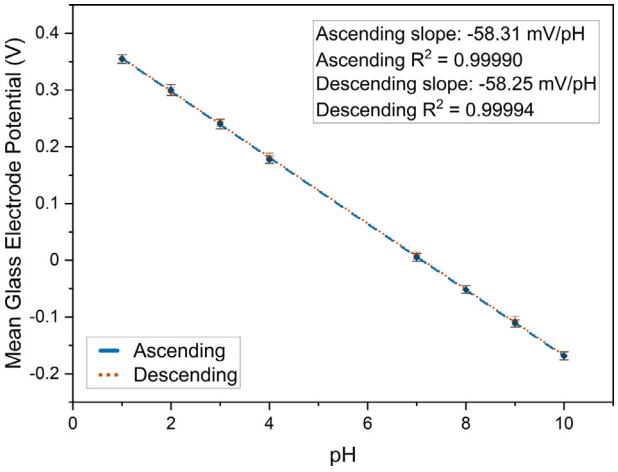

Fig. 6. pH calibration curves for a commercial glass pH electrode using a 4P SPRE electrode in buffer solutions measured in both ascending (blue, dash) and descending (orange, dot) pH order. The error bars represent the standard deviation of each measurement calculated from the data collected over a 5 min period.

The electrodes were not conditioned prior to measurement and demonstrated average hydration times consistent with earlier findings in this study of 13.3, 18.3 and 91 min in creek water, coffee, and tap water, respectively. Table 2 shows that the electrodes maintain lifetimes similar to those for the earlier lifetime testing in 0.1 M K_2SO_4 (Section 3.2) and that the working potential and variation are well within the working definition from Shitanda et al. [27] of −45 ± 30 mV vs. SCE in each solution during their lifetimes.

It is notable that the average working potential for the electrodes in all three solutions was around 7 mV lower than the operating potential range demonstrated for 4P SPREs in Table 1, and there was a corresponding increase in potential variation. These differences in potential may be due to sample variance and the increased complexity of the analyte solutions compared to laboratory standards, and as such the failure point for electrodes in these tests was redefined to be once the potential had drifted permanently above −40 mV. It should also be noted that the potentials in these three analytes are similar to the electrode responses to the more challenging interference species (such as in the acid/base and redox tests, Section 3.3). Sample variation, as well as differences in solution ion concentration and the presence of organic material in the solutions, may also explain the longer hydration times and shorter lifetimes in tap water compared to coffee or creek water.

The overall conclusion from these tests is that, in both laboratory standards and solutions of unknown composition, the electrolyte and PDMS junction layers in the 4P SPREs allow the electrodes to maintain a sufficiently stable potential throughout their decent working lifetime for practical and commercial applications and thus the SPREs described in this work are suitable for electroanalytical use outside of a laboratory environment.

Table 3
pH measurements of 6 common solutions using a commercial pH probe with an internal reference and meter, as well as using an external SPRE with a potentiostat.

Sample	pH probe with internal RE	pH probe using 4P SPRE
Coffee	5.04	4.89
Creek Water	7.28	7.53
Milk	6.53	6.45
Orange Juice	3.62	3.58
Carbonated Tap Water	4.06	4.29
Tap Water	6.90	7.08

3.6. pH calibration

To demonstrate their suitability for ISE applications, a 4P SPRE preconditioned in 0.1 M KCl was combined with a commercial glass pH indicator electrode. Variation in the mean glass pH electrode potential response in a series of buffers from pH 1–10 is shown in Fig. 6. There was no significant hysteresis observed when the measurement was conducted in both the ascending (pH 1–10) and descending (pH 10–1) directions, and negligible difference between the resulting linear calibration curves. The average calibration curve was near-Nernstian with a slope of −58.28 mV/pH [42] across the measured pH range, indicating suitable SPRE stability for reliable pH measurement.

The average calibration curve was used to measure the pH of six common solutions to compare against measurements from the commercial pH probe with the internal RE, as shown in Table 3. The results from both devices show good agreement, with the largest differences in pH being for the creek water (0.25) and carbonated tap water (0.23) samples; however, degassing in the period between measurements is a suspected major contributor to this discrepancy. Further work is required to determine the SPRE's suitability for measuring pH in a full range of solutions and any considerations for long-term monitoring, such as biofouling, but

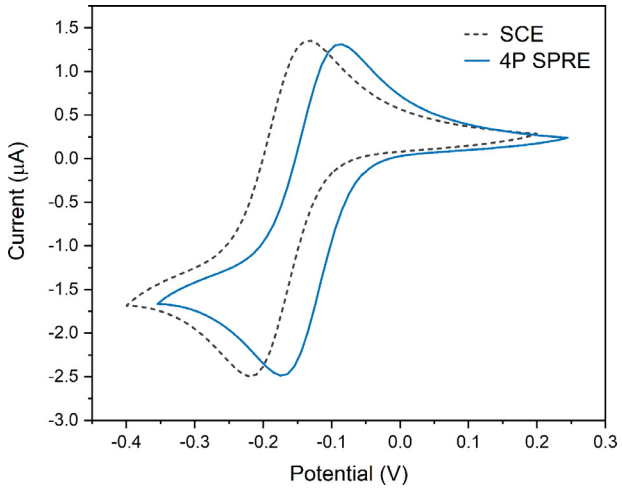

Fig. 7. Cyclic voltammograms for a 4P SPRE (solid blue line) and a commercial SCE (dashed black line) performed at 50 mV/s using a glassy carbon WE in a 2 mM $[Ru(NH_3)_6]Cl_3$ with a 0.1 M KNO_3 supporting electrolyte.

these results demonstrate that the SPRE is at least well suited to intermittent measurements in a variety of solutions.

3.7. Cyclic voltammetry

The voltammetric performance of a 4P SPRE was investigated through a cyclic voltammogram using a glassy carbon WE (1 mm diameter) in a 2 mM $[Ru(NH_3)_6]Cl_3$ solution with a 0.1 M KNO_3 supporting electrolyte. The performance of the SPRE was similar to a commercial SCE (Fig. 7), with peaks shifted by exactly 45 mV due to the potential difference between the SCE and Ag/AgCl systems, and ΔE_p (the peak-to-peak separation potential) was 89.84 mV for both electrodes. The SPRE peak current magnitudes were slightly lower than for the SCE (0.01 μA for reduction, 0.04 μA for oxidation). Although it is possible to use a pseudo-RE in many voltammetric measurements, a standard SPRE may be preferred to maintain reproducibility where the inability to calculate the potential of pseudo-REs as well as their significant potential shifts render them unsuitable, especially for continuous monitoring in unknown or remote working environments where an internal standard cannot be used to verify the pseudo-RE potential [15,43]. These results indicate that the 4P SPRE may be suitable for voltammetric measurements, including in a printed multi-sensor device, although further work is needed to establish their performance in a wider variety of environments.

4. Conclusion

Screen-printed, flexible planar Ag/AgCl reference electrodes including a PVAc/KCl electrolyte layer and PDMS junction membrane were fabricated successfully at low curing temperatures. Electrode failure was caused by loss of the KCl electrolyte, as confirmed by SEM and EDS analysis. The balanced permeability and hydrophobicity of the additional PDMS junction membrane in combination with the offset reservoir dramatically increased electrode lifetime and stability by improving electrolyte retention, with the best performing electrodes demonstrating a lifetime of up to 27 days with less than ± 3 mV potential variation and very low potential drift of 0.25 mV/day during this time.

This best-performing electrode type was tested using OCP and impedance in different interfering solutions. The electrode potential was stable when exposed to SO_4^{2-}, I^-, Br^-, and F^- anions, as well as Li^+, Na^+, and K^+ alkali cations. The SPRE potential was also stable across pH 4–10, with only a minor potential shift in extreme conditions, *i.e.* highly acidic 10% H_2SO_4 (−10 mV) and highly alkaline 10% KOH (+ 5 mV). The potential was constant in the presence of reducing species, but oxidant by-products caused significant potential change. The $[Cl^-]$ susceptibility was −0.31 ± 0.15 mV/pCl, which is low when compared with previous studies.

Hydration times for fresh SPREs were less than 1 h in all test conditions and reached as low as 5 min in some solutions. This rapid hydration was accompanied by a fast decrease in electrochemical impedance to ∼ 15 kΩ.

The developed SPREs indicated suitability for both potentiometric and voltammetric applications, and could be integrated readily into a fully printed multi-sensor device. A near-Nernstian calibration curve was obtained in combination with a commercial pH probe, while sample measurements showed good agreement with a commercial pH meter. The electrode also performed similarly to a commercial SCE in cyclic voltammetry measurements.

The short hydration time, long lifetime, negligible drift, and low sensitivity to interfering species demonstrate that the low-cost, flexible SPREs developed in this study are highly suitable for integration into a printed sensor platform for electroanalytical systems. The stability and lifetime of the electrodes in real solutions points towards on-site applications when combined with suitable ISE or voltammetric electrodes with similar stability. Disposable sensors with a lifetime of several weeks without maintenance would enable non-laboratory personnel to conduct accurate analysis on-site. Further development is required to increase the lifetime of the electrodes to make them more suitable for continuous online analysis.

Declaration of Competing Interest

The authors declare that they have no known competing financial interests or personal relationships that could have appeared to influence the work reported in this paper.

Credit authorship contribution statement

Rebecca C. Dawkins: Conceptualization, Methodology, Software, Validation, Formal analysis, Data curation, Investigation, Writing – original draft, Writing – review & editing, Visualization. **Dingchen Wen:** Conceptualization, Investigation, Methodology. **Judy N. Hart:** Supervision, Writing – review & editing. **Mikko Vepsäläinen:** Supervision, Conceptualization, Methodology, Resources, Writing – review & editing, Funding acquisition.

Acknowledgments

This work was supported by the Department of Education and Training of the Australian Government via a Postgraduate Research Training Program Scholarship and the CSIRO via a Top-Up Scholarship to RCD. Appreciation is also extended to CSIRO colleagues Mr. Mike Horne, Mrs. Luda Malishev, Mr. David Macedo, and Mr. Cameron Davidson for their assistance.

Supplementary materials

Supplementary material associated with this article can be found, in the online version, at doi:10.1016/j.electacta.2021.139043.

References

[1] A. Salam, Internet of things in water management and treatment, in: A. Salam (Ed.), Internet of Things, Springer Nature, Switzerland, 2020, pp. 273–298, doi:10.1007/978-3-030-35291-2_9. AG.

[2] A. Jang, J.H. Lee, P.R. Bhadri, S.A. Kumar, W. Timmons, F.R. Beyette, I. Papautsky, P.L. Bishop, Miniaturized redox potential probe for *in situ* environmental monitoring, Environ. Sci. Technol. 39 (2005) 6191–6197, doi:10.1021/es050377a.

[3] M.H. Banna, H. Najjaran, R. Sadiq, S.A. Imran, M.J. Rodriguez, M. Hoorfar, Miniaturized water quality monitoring pH and conductivity sensors, Sens. Actuators B Chem. 193 (2014) 434–441, doi:10.1016/J.SNB.2013.12.002.
[4] D.J.G. Ives, G.J. Janz, Reference Electrodes: Theory and Practice, Academic Press Inc., New York, 1961.
[5] M. Sophocleous, J.K. Atkinson, A review of screen-printed silver/silver chloride (Ag/AgCl) reference electrodes potentially suitable for environmental potentiometric sensors, Sens. Actuators A Phys. 267 (2017) 106–120, doi:10.1016/J.SNA.2017.10.013.
[6] J. Wang, Real-time electrochemical monitoring: toward green analytical chemistry, Acc. Chem. Res. 35 (2002) 811–816, doi:10.1021/ar010066e.
[7] L. Manjakkal, D. Shakthivel, R. Dahiya, Flexible printed reference electrodes for electrochemical applications, Adv. Mater. Technol. 3 (2018) 1–8, doi:10.1002/admt.201800252.
[8] W.Y. Liao, T.C. Chou, Fabrication of a planar-form screen-printed solid electrolyte modified Ag/AgCl reference electrode for application in a potentiometric biosensor, Anal. Chem. 78 (2006) 4219–4223, doi:10.1021/ac051562.
[9] Ł. Tymecki, E.E.E. Zwierkowska, R. Koncki, Screen-printed reference electrodes for potentiometric measurements, Anal. Chim. Acta 526 (2004) 3–11, doi:10.1016/j.aca.2004.08.056.
[10] H. Suzuki, H. Shiroishi, Microfabricated liquid junction Ag /AgCl reference electrode and its application to a one-chip potentiometric sensor, Structure 71 (1999) 5069–5075, doi:10.1021/ac990437t.
[11] A. Hayat, J. Marty, Disposable screen printed electrochemical sensors: tools for environmental monitoring, Sensors 14 (2014) 10432–10453, doi:10.3390/s140610432.
[12] A. Simonis, H. Lüth, J. Wang, M.J. Schöning, New concepts of Miniaturised reference electrodes in silicon technology for potentiometric sensor systems, Sens. Actuators B Chem. 103 (2004) 429–435, doi:10.1016/J.SNB.2004.04.072.
[13] J.K. Atkinson, An evaluation and comparison of cross-sensitivities of various different types of screen printed Ag/AgCl reference electrodes, in: Proceedings of the International Conference on Electronics Packaging IMAPS All Asia Conference ICEP-IAAC, 2018, pp. 299–303, doi:10.23919/ICEP.2018.8374308.
[14] S. Søpstad, E.A. Johannessen, F. Seland, K. Imenes, Long-term stability of screen-printed pseudo-reference electrodes for electrochemical biosensors, Electrochim. Acta 287 (2018) 29–36, doi:10.1016/j.electacta.2018.08.045.
[15] G. Inzelt, Pseudo-reference electrodes, in: G. Inzelt, A. Lewenstam, F. Scholz (Eds.), Handbook of Reference Electrodes, Springer Berlin Heidelberg, Berlin, Heidelberg, 2013, pp. 331–332, doi:10.1007/978-3-642-36188-3_14.
[16] J. Soto, I. Campos, R. Martínez-Máñez, Monitoring wastewater treatment using voltammetric electronic tongues, in: S.C. Mukhopadhyay, A. Mason (Eds.), Smart Sensors Real-Time Water Quality Monitoring, Springer Berlin Heidelberg, Berlin, Heidelberg, 2013, pp. 65–103, doi:10.1007/978-3-642-37006-9_4.
[17] I. Campos, M. Alcañiz, D. Aguado, R. Barat, J. Ferrer, L. Gil, M. Marrakchi, R. Martínez-Mañez, J. Soto, J.L. Vivancos, A voltammetric electronic tongue as tool for water quality monitoring in wastewater treatment plants, Water Res. 46 (2012) 2605–2614, doi:10.1016/J.WATRES.2012.02.029.
[18] D. Diamond, E. McEnroe, M. McCarrick, A. Lewenstam, Evaluation of a new solid-state reference electrode junction material for ion-selective electrodes, Electroanalysis 6 (1994) 962–971, doi:10.1002/elan.1140061108.
[19] Z. Mousavi, K. Granholm, T. Sokalski, A. Lewenstam, An analytical quality solid-state composite reference electrode, Analyst 138 (2013) 5216, doi:10.1039/c3an00852e.
[20] A. Jasiński, M. Urbanowicz, M. Guziński, M. Bocheńska, Potentiometric solid-contact multisensor system for simultaneous measurement of several ions, Electroanalysis 27 (2015) 745–751, doi:10.1002/elan.201400585.
[21] K. Granholm, Z. Mousavi, T. Sokalski, A. Lewenstam, Analytical quality solid-state composite reference electrode manufactured by injection molding, J. Solid State Electrochem. 18 (2014) 607–612, doi:10.1007/s10008-013-2294-x.
[22] W. Vonau, W. Oelßner, U. Guth, J. Henze, An all-solid-state reference electrode, Sens. Actuators B Chem. 144 (2010) 368–373, doi:10.1016/J.SNB.2008.12.001.
[23] A.W.J. Cranny, J.K. Atkinson, Thick film silver-silver chloride reference electrodes, Meas. Sci. Technol. 9 (1998) 1557–1565, doi:10.1088/0957-0233/9/9/027.
[24] M. Komoda, I. Shitanda, Y. Hoshi, M. Itagaki, Fabrication and characterization of a fully screen-printed Ag/AgCl reference electrode using silica gel inks exhibiting instantaneous usability and long-term stability, Electrochemistry 87 (2019) 65–69, doi:10.5796/electrochemistry.18-00075.
[25] A. Simonis, M. Dawgul, H. Lüth, M.J. Schöning, Miniaturised reference electrodes for field-effect sensors compatible to silicon chip technology, Electrochim. Acta 51 (2005) 930–937, doi:10.1016/j.electacta.2005.04.063.
[26] J.K. Atkinson, M. Glanc, P. Boltryk, M. Sophocleous, E. Garcia-Breijo, An investigation into the effect of fabrication parameter variation on the characteristics of screen printed thick film silver/silver chloride reference electrodes, Microelectron. Int. 28 (2011) 49–53, doi:10.1108/13565361111127368.
[27] I. Shitanda, H. Kiryu, M. Itagaki, Improvement in the long-term stability of screen-printed planar type solid-state Ag/AgCl reference electrode by introducing poly(dimethylsiloxane) liquid junction, Electrochim. Acta 58 (2011) 528–531, doi:10.1016/j.electacta.2011.09.086.
[28] M. Glanc, M. Sophocleous, J.K. Atkinson, E. Garcia-Breijo, The effect on performance of fabrication parameter variations of thick-film screen printed silver/silver chloride potentiometric reference electrodes, Sens. Actuators A Phys. 197 (2013) 1–8, doi:10.1016/J.SNA.2013.03.036.
[29] A. Kisiel, A. Michalska, K. Maksymiuk, Plastic reference electrodes and plastic potentiometric cells with dispersion cast poly(3,4-ethylenedioxythiophene) and poly(vinyl chloride) based membranes, Bioelectrochemistry 71 (2007) 75–80, doi:10.1016/j.bioelechem.2006.09.006.
[30] R. Mamińska, A. Dybko, W. Wróblewski, All-solid-state Miniaturised planar reference electrodes based on ionic liquids, Sens. Actuators B Chem. 115 (2006) 552–557, doi:10.1016/j.snb.2005.10.018.
[31] S. Alva, L.Y. Heng, M. Ahmad, Optimization of screen printed reference electrode based on charge balance and poly (butyl acrylate) photocurable membrane, Int. J. Innov. Mech. Eng. Adv. Mater. 2 (2016) 10, doi:10.22441/ijimeam.2016.1.002.
[32] F. Pargar, H. Kolev, D.A. Koleva, K. van Breugel, Potentiometric response of Ag/AgCl chloride sensors in model alkaline medium, Adv. Mater. Sci. Eng. 2018 (2018) 1–12, doi:10.1155/2018/8135492.
[33] I. Shitanda, M. Komoda, Y. Hoshi, M. Itagaki, An instantly usable paper-based screen-printed solid-state KCl/Ag/AgCl reference electrode with long-term stability, Analyst 140 (2015) 6481–6484, doi:10.1039/C5AN00617A.
[34] J.K. Atkinson, M. Glanc, M. Prakorbjanya, M. Sophocleous, R.P. Sion, E. Garcia-Breijo, Thick film screen printed environmental and chemical sensor array reference electrodes suitable for subterranean and subaqueous deployments, Microelectron. Int. 30 (2013) 92–98, doi:10.1108/13565361311314485.
[35] J.M. Watson, M.G. Baron, The behavior of water in poly(dimethylsiloxane), J. Membr. Sci. 110 (1996) 47–57, doi:10.1016/0376-7388(95)00229-4.
[36] J.C. McDonald, D.C. Duffy, J.R. Anderson, D.T. Chiu, H. Wu, O.J.A. Schueller, G.M. Whitesides, Fabrication of microfluidic systems in poly(dimethylsiloxane), Electrophoresis 21 (2000) 27–40, doi:10.1002/(SICI)1522-2683(20000101).
[37] H. Zhang, M. Chiao, Anti-fouling coatings of poly(dimethylsiloxane) devices for biological and biomedical applications, J. Med. Biol. Eng. 35 (2015) 143–155, doi:10.1007/s40846-015-0029-4.
[38] A. Simonis, H. Lüth, J. Wang, J. Schöning, Strategies of Miniaturised reference electrodes integrated in a silicon based “one chip” pH Sensor, Sensors 3 (2003) 330–339, doi:10.3390/s30900330.
[39] T.J. Smith, K.J. Stevenson, Reference electrodes, in: Handbook of Electrochemistry, Elsevier, 2013, pp. 73–110, doi:10.1361/asmhba0003799.
[40] M. Glanc-Gostkiewicz, M. Sophocleous, J.K. Atkinson, E. Garcia-Breijo, Performance of Miniaturised thick-film solid state pH sensors, Sens. Actuators A Phys. 202 (2013) 2–7, doi:10.1016/j.sna.2013.04.012.
[41] M. Sophocleous, M. Glanc-Gostkiewicz, J.K. Atkinson, E. Garcia-Breijo, An experimental analysis of Thick-Film solid-state reference electrodes, in: Proceedings of the IEEE Sensors, 2012, pp. 12–15, doi:10.1109/ICSENS.2012.6411137.
[42] D.J. Graham, B. Jaselskis, C.E. Moore, Development of the glass electrode and the pH response, J. Chem. Educ. 90 (2013) 345–351, doi:10.1021/ed300246x.
[43] N. Elgrishi, K.J. Rountree, B.D. McCarthy, E.S. Rountree, T.T. Eisenhart, J.L. Dempsey, A practical beginner's guide to cyclic voltammetry, J. Chem. Educ. 95 (2018) 197–206, doi:10.1021/acs.jchemed.7b00361.